Applied Catalysis B: Environmental 84 (2008) 497-504

Mechanistic aspects of N_2O and N_2 formation in NO reduction by NH_3 over Ag/Al_2O_3: the effect of O_2 and H_2

V.A. Kondratenko[*1], U. Bentrup[1], M. Richter[1], T.W. Hansen[2], E. V. Kondratenko[1]

[1]Leibniz-Institut für Katalyse e.V. an der Universität Rostock Außenstelle Berlin, Richard-Willstätter-Str.12, D-12489, Berlin, Germany
[2]Fritz-Haber-Institut der Max-Planck-Gesellschaft, Faradayweg 4-6, D-14195 Berlin, Germany

[*] Corresponding author: e-mail Vita.Kondratenko@catalysis.de,

Received 15 February 2008; revised 30 April 2008; accepted 10 May 2008. Available online 22 May 2008..

Abstract

A mechanistic scheme of N_2O and N_2 formation in the selective catalytic reduction of NO with NH_3 (NH_3-SCR) over a Ag/Al_2O_3 catalyst in the presence and absence of H_2 and O_2 was developed by applying a combination of different techniques: transient experiments with isotopic tracers in the temporal analysis of products (TAP) reactor, HRTEM, in situ UV/vis and in situ FTIR spectroscopy. Based on the results of transient isotopic analysis and in situ IR experiments, it is suggested that N_2 and N_2O are formed via direct or oxygen-induced decomposition of surface NH_2NO species. These intermediates originate from NO and surface NH_2 fragments. The latter NH_2 species are formed upon stripping of hydrogen from ammonia by adsorbed oxygen species, which are produced over reduced silver species from NO, N_2O and O_2. The latter is the dominant supplier of active oxygen species. Lattice oxygen in oxidized AgO_x particles is less active than adsorbed oxygen species particularly below 623 K. The previously reported significant diminishing of N_2O production in the presence of H_2 is ascribed to hydrogen-induced generation of metallic silver sites, which are responsible for N_2O decomposition.

Keywords: NH_3-SCR, ammonia, reaction mechanism, TAP reactor, silver, nitric oxide, nitrous oxide

1. Introduction

A negative ecological effect of nitrogen oxides (NO_x) excites enhanced efforts for the development of environmental friendly solutions for decreasing NO_x emissions. Selective catalytic reduction of NO_x with NH_3 (NH_3-SCR) is considered as an efficient way for NO_x abatement from mobile diesel engines in the frame of an urea-SCR technology. Similar to selective reduction of NO_x by hydrocarbons (HC-SCR) over Ag/Al_2O_3 [1], the catalyst light-off temperature is significantly decreased (down to 473 K), when H_2 is added to NO- and NH_3-containing feeds. Such a low-temperature operation regime meets the requirements for application in mobile diesel engines. The boosting effect of H_2 on NO reduction both with hydrocarbons and ammonia may indicate that H_2 influences the same reaction steps in the SCR reaction, for example generation of active sites or activation of NO_x. A deep understanding of the remarkable effect of H_2 on the SCR reaction over Ag/Al_2O_3 will be useful not only for further improvement of the Ag/Al_2O_3 catalysts but possibly also for the development of catalytic materials operating effectively without added H_2. Different approaches for the explanation of the role of H_2 in the SCR reaction are discussed in the literature by now. The boosting effect of H_2 is ascribed to i) promoting of formation of $Ag_n^{\delta+}$ clusters [1-4], essential for certain reaction pathways; ii) the initiation of radical reactions [5, 6]; iii) the formation of intermediate surface species like cyanides or nitrites and nitrates [5, 7]. Satokawa et al. [1, 2, 4] have concluded on the basis of in situ UV/vis studies that H_2 facilitates the formation of moderately agglomerated $Ag_n^{\delta+}$ clusters, which are responsible for activation of hydrocarbons [3, 8] or also promote dissociation of NO or O_2 [9, 10]. However, in situ UV/vis spectra recorded during analysis of decane-SCR-NO_x reaction performed by Sazama et al. [5] have shown that the formation of $Ag_n^{\delta+}$ clusters containing less

than 8 Ag atoms takes place even in absence of H_2. A sharp decrease in NO_x conversion rate caused by removing of hydrogen from the feed in their experiments did not lead to a respective decay in the surface coverage by $Ag_n^{\delta+}$ clusters. Co-feeding of CO instead of H_2 in the HC-SCR also resulted in the formation of $Ag_n^{\delta+}$ clusters [11]. However, no promoting effect of CO was detected. Hence, it was concluded that the activity increase of silver catalyst in selective catalytic reduction of NO_x in the presence of H_2 could not be ascribed to the facilitated formation of $Ag_n^{\delta+}$ clusters. It was assumed that hydrogen initiates radical-type reactions and increases in this way the rate of all reaction steps. According to the reaction scheme developed in [5], hydrogen dissociation over silver catalyst leads to the formation of silver hydride. The latter reacts with oxygen to hydroperoxy radicals, which in turn oxidize NO to NO_2 forming hydroxyl radicals. The both types of radical species interact with hydrocarbons yielding their oxo derivatives - formate (acrylate). An increase in surface coverage by these species during HC-SCR in the presence of gas-phase H_2 was detected by FTIR [5]. Shimizu and Satsuma [6] observed O_2^- (super oxide) ion on the surface of Ag/Al_2O_3 after NH_3-SCR performed in the presence of H_2 at 423 K by ESR spectroscopy. The authors have suggested that these oxygen ions participate in NH_x formation from ammonia and oxidation of NO to NO_2. The latter reacts with NH_x yielding N_2 and H_2O.

Hydrogen also promotes a complex transformation of CN intermediates connected with Ag^+ into NCO species bound to Al sites of support [5], earlier shown to be a relevant reaction step of NO_x-SCR by in situ FTIR studies of NO reduction with ethanol in the presence of oxygen [12]. Additionally, hydrogen reduces the concentration of surface nitrates [7], which block active sites for the SCR reaction over Ag/Al_2O_3 below 523 K.

The suggested mechanistic concepts are still controversial and in some aspects partial. For example, the reaction pathways leading to N_2O, a possible undesired side-product of this reaction, are scarcely investigated. As reported in our previous publication [10], the formation of N_2O in the SCR reaction over Ag/Al_2O_3 is significantly decreased in the presence of hydrogen. This is especially valid for low-temperature operation. From an environmental point of view, the decrease of N_2O emission is highly desirable, since N_2O contributes to global warming and ozone depletion in the upper atmosphere. Its potential to warm up the atmosphere is 310 times stronger as compared to CO_2. Besides the above environmental aspects, mechanistic understanding of reaction pathways of N_2O formation and decomposition may be helpful not only for the suppression of the N_2O emissions in NH_3-SCR over Ag-containing catalysts but also over other catalytic materials and even for other chemical processes like ammonia oxidation to nitric oxide or adipic acid production.

From the above background, the present study was aimed at elucidating of reaction pathways influencing N_2O emissions in the NH_3-SCR reaction over Ag/Al_2O_3 in the presence of O_2 and H_2. For this purpose, we investigated the origins of N_2O formation and its decomposition using isotopic tracers ($^{15}NH_3$) in the temporal analysis of products (TAP-2) reactor. In order to derive insights into the redox properties of AgO_x species and into possible reactive surface intermediates, the catalysts have been characterized using HRTEM, in situ FTIR and in situ UV/vis spectroscopy. In this way, the mechanistic knowledge obtained from the transient studies can be directly related to surface intermediates and to the state of silver species under reaction conditions. This fundamental knowledge may be important for designing of catalytic materials preventing N_2O formation in the NO_x abatement from mobile diesel engines in the frame of an urea-SCR technology.

2. Experimental

2.1. Catalyst preparation

Details on the preparation procedure of Ag/Al_2O_3 catalysts have been described elsewhere [13]. Shortly, alumina hydrate powder (Disperal P2, CONDEA) was dispersed in water under intense stirring at room temperature for at least 30 min. Hereafter, an appropriate amount of 1M $AgNO_3$ solution was added to the sol to achieve the desired Ag content. The immediately formed gel was filtered and dried at 393 K for 2 h. The obtained powder was compressed to pellets and subsequently crushed yielding samples with mesh sizes (ASTM) from 42 to 24 (350-710 μm). A sample used in the present study (designated as $2Ag/Al_2O_3$) had an Ag loading of 1.73 wt.%. The silver content was determined by elemental analysis (OES-ICP). The texture of the catalyst was similar to that of the alumina support. After calcination in air at 873 K for 2 h the support had a γ-Al_2O_3 phase structure with a BET surface area of 235 $m^2 \cdot g^{-1}$, a pore volume of 0.43 $cm^3 \cdot g^{-1}$ and an average pore diameter of 5.2 nm.

2.2 Transient experiments

Transient studies were performed in the temporal analysis of products (TAP-2) reactor. The TAP-2 reactor system has been described in detail elsewhere [14]. The catalyst (ca. 200 mg; d_p = 250-355 μm) was packed between two layers of quartz of the same particle size in the micro reactor made of quartz. Before transient experiments the catalyst was pre-treated at ambient pressure either in an O_2 flow (50 cm^3_{STP}/min) at 823 K for 2 h or in a flow of H_2 (H_2/Ar = 5/95, 50 cm^3_{STP}/min) at 373 K for 30 min. The pre-treated catalysts are denoted as pre-oxidized and pre-reduced, respectively. After the treatment, the catalyst was exposed to vacuum (*ca*. 10^{-5} Pa) and pulse experiments were carried out in the temperature range between 423 and 723 K with 100 K intervals.

Transient experiments were performed using O_2/Xe = 1/1, $^{15}NH_3/^{14}NO$/Ne = 1/1/1 and $^{15}NH_3/^{14}NO/H_2$/Ne = 1/1/10/1 mixtures. The pulse size was kept for all experi-

ments in the range of $5 \cdot 10^{14}$ - $9 \cdot 10^{14}$ molecules enabling operation in the Knudsen diffusion regime and, therefore, minimizing gas-phase interactions. The following gases were applied: H_2 (5.0), Ne (4.5), Xe (4.0), O_2 (4.5), ^{14}NO (2.5) and $^{15}NH_3$ (99.9% atoms of ^{15}N). Isotopically labeled ammonia was purchased from ISOTEC. The following atomic mass units (AMUs) were used for mass-spectroscopic identification of different compounds: 132 (Xe), 46 ($^{14}NO_2$, $^{15}N_2O$), 45 ($^{14}N^{15}NO$), 44 ($^{14}N_2O$), 32 (O_2), 31 (^{15}NO, $H^{14}NO$), 30 ($^{14}N_2O$, ^{14}NO, $^{15}N_2$), 29 ($^{14}N^{15}N$), 28 ($^{14}N_2O$, $^{14}N_2$), 20 (Ne), 18 (H_2O, $^{15}NH_3$), 17 ($^{14}NH_3$, $^{15}NH_3$, H_2O), and 2 (H_2). For each AMU, pulses were repeated 10 times and averaged to improve the signal-to-noise ratio.

The concentration of feed components and reaction products was determined from the respective AMUs using standard fragmentation patterns and sensitivity factors, which arise from the different ionization probabilities of individual compounds. The relative sensitivities were determined as a ratio of the areas under the response signals of each compound related to the area under the response signal of inert gas. The respective areas were corrected according to the contribution of fragmentation patterns of other compounds to the measured AMU signal. The fragmentation patterns and respective sensitivities of feed components and reaction products were determined from separate calibration experiments, where a mixture of the gas and inert standard was pulsed in the reactor filled only with SiO_2 particles. It was assumed that there is no difference in the calibration values between isotopically labeled and non-labeled compounds.

2.3. UV/vis and FTIR experiments

In situ UV/vis diffuse reflectance spectra were taken on a Varian Cary 400 UV/vis spectrophotometer as described in [15]. A stainless steel reaction chamber with quartz windows was used in combination with diffuse reflectance attachment (DRA of Harrick) for measurements performed under gas feed up to 823 K. The unloaded alumina served as reference. In situ UV/vis spectra were measured in reflectance mode and converted into the Kubelka-Munk function, $F(R_\infty)$, using implemented routine GRAMS32 (Galactic). Reduction/oxidation measurements were carried out in a quasi temperature-programmed mode as follows. Before spectra recording the catalyst was treated with O_2/N_2 mixture (5/95, 25 cm^3_{STP}/min) at 773 K for 30 min. After cooling, a first spectrum was taken at room temperature. Subsequently, the flow was switched to an H_2/N_2 flow (5/95, 25 cm^3_{STP}/min) and the sample was heated in steps of 20 K up to 823 K and kept at this temperature for 30 min, before returning to room temperature under flow of N_2. Oxidation was started at room temperature with the same flow that served for pre-treatment. Spectra were recorded every 50 K up to 823 K, keeping the sample at this temperature for 30 min. After completion of this cycle, a final spectrum was recorded at room temperature again.

FTIR spectra were recorded by means of a Bruker IFS 66 spectrometer using a reaction cell with CaF_2 windows, which was connected to a gas dosing - evacuation system. Adsorption experiments were performed on self-supporting wafers (m = 50 mg, d = 20 mm) of the catalyst powder.

The catalyst was either pre-oxidized in air (60 $cm^3 \cdot min^{-1}$) at 573 K for 1 h or pre-reduced by treating the sample with 5 vol.% H_2/Ar (60 $cm^3 \cdot min^{-1}$) at 573 K for 1 h. After these pretreatment procedures, the interaction of the catalyst with the reactant mixture (100 $cm^3 \cdot min^{-1}$) at 423 K was monitored for 90 min. The composition of the reactant mixture was 0.04 vol.% NO/0.04 vol.% NH_3/4 vol.% O_2/ 1vol.% H_2 balanced by inert gas. For one experiment a gas mixture of 0.09 vol.% NO/2 vol.% O_2 was pre-adsorbed for 30 min and, then, the catalyst was exposed to 1 vol.% H_2/Ar or 0.4 vol.% NH_3/Ar for 60 min.

2.4. HRTEM measurements

HRTEM measurements were carried out in a Philips CM200 FEG transmission electron microscope equipped with a Gatan Tridiem image filter. During storage and transportation, the samples were kept in ampoules under nitrogen atmosphere. Prior to imaging, the ampoules were opened and the samples were crushed using a mortar and pestle. The resulting powder was dispersed on a copper TEM grid covered with a holey carbon film. Images were acquired and analyzed using DigitalMicrograph™ from Gatan Inc.

3. Results and discussion

The following three sections describe the results of physical and chemical characterization of $2Ag/Al_2O_3$ catalytic material as well as of transient isotopic analysis. Finally, a detailed mechanistic concept of nitrogen and nitrous oxide formation in the NO-NH_3-O_2-H_2 interactions is suggested and discussed.

3.1 Catalyst morphology and redox behavior of AgOx species

The influence of the catalyst treatment on the oxidation state of silver on the catalyst surface was studied by XRD and HRTEM. XRD measurements showed that no silver-containing crystalline phases exist in the catalyst. Nano-sized silver particles were identified on the catalyst surface by means of HRTEM analysis. Since this method does not allow detecting of Ag_n^+ clusters on atomic level, the following discussion is related to nano-sized AgO_x species. In order to check, if the size of these species is influenced by reaction conditions, HRTEM images of oxi

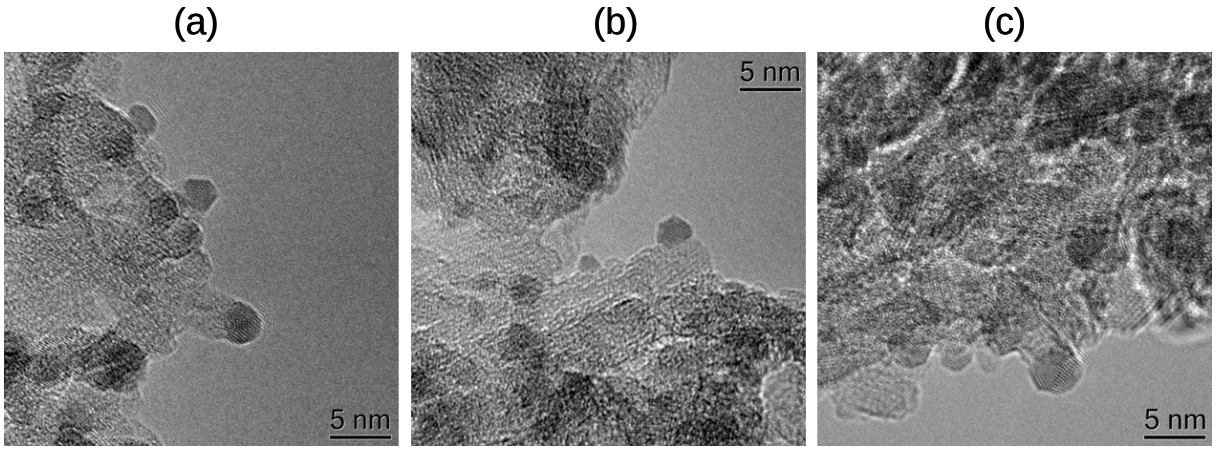

Fig. 1: TEM images of $2Ag/Al_2O_3$ pretreated under different conditions: a) calcined at 773 K in air for 2 h, b) reduced at 373 K by hydrogen (H_2/Ar = 5/95, 50 cm^3_{STP}/min) for 2 h and c) reduced at 473 K by hydrogen (H_2/Ar = 5/95, 50 cm^3_{STP}/min) for 2 h.

dized and reduced samples were recorded. Fig. 1 shows TEM images of oxidized $2Ag/Al_2O_3$ (calcination at 773 K in air for 2 h (Fig. 1a)), $2Ag/Al_2O_3$ reduced at 373 K (Fig. 1b) and 473 K (Fig. 1c) by hydrogen (H_2/Ar = 5/95, 50 cm^3_{STP}/min) for 2 h. One can see that the average diameter of nano-sized silver particles does not depend on the type of treatment and amounts to ca. 3 nm. However, the treatment influences the oxidation state of silver. Silver exists in the form of polycrystalline silver oxide (Ag_2O) on the pre-oxidized sample. On the sample treated in hydrogen, metallic Ag nano clusters of the same size could be detected by converging beam diffraction on selected particles. This confirms that dispersion of Ag during H_2-reduction of nano-sized Ag_2O does not proceed to an extent that is recognizable by HRTEM. Clusters that undergo dispersion and agglomeration processes on the Al_2O_3 surfaces comprise 4 to 8 silver ions and their formation can be obtained from EXAFS and UV/vis analysis Thus, the existence of $Ag_n^{\delta+}$ clusters on a 2 wt.% Ag/Al_2O_3 catalyst after pre-reduction at 573 K is reported to occur [16]. Redispersion of such small clusters to Ag^+ under oxidizing conditions is possible as followed from EXAFS measurements [16]. Breen et al. [17] reported that an increase in the Ag-Ag coordination is observed from EXAFS data, when the catalyst is exposed to SCR reaction conditions at 723 K using C_8H_{18} as reductant. This effect is more pronounced if switching to reducing conditions using 8 % H_2/He at the same temperature. Because no Ag-O coordination is retained under these reducing conditions, it can be concluded that all Ag_xO is completely reduced [17].

Reversible reduction/reoxidation of Ag_2O/Ag over $2Ag/Al_2O_3$ was confirmed by in situ UV/vis spectroscopic analysis. In these experiments, UV/vis spectra were recorded under oxidizing (O_2/N_2 = 5/95, 25 cm^3_{STP}/min) or reducing (H_2/N_2 = 5/95, 25 cm^3_{STP}/min) conditions at different reaction temperatures. Fig. 2 (a) and (b) exemplifies UV/vis spectra recorded during reduction of pre-oxidized $2Ag/Al_2O_3$ by a mixture of H_2 and N_2 and during oxidation of previously reduced silver catalyst by O_2 diluted with N_2,

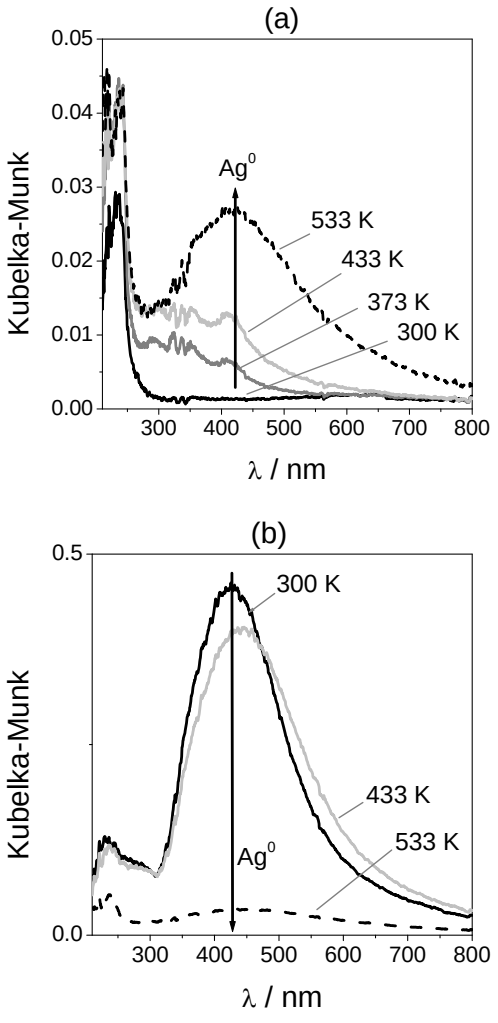

Fig. 2: In situ UV/vis spectra: a) during reduction of oxidized $2Ag/Al_2O_3$ in a H_2 flow (H_2/N_2=5/95, 25 cm^3_{STP}/min) at different temperatures; b) during reoxidation of reduced $2Ag/Al_2O_3$ in an O_2 flow (O_2/N_2=5/95, 25 cm^3_{STP}/min) at different temperatures.

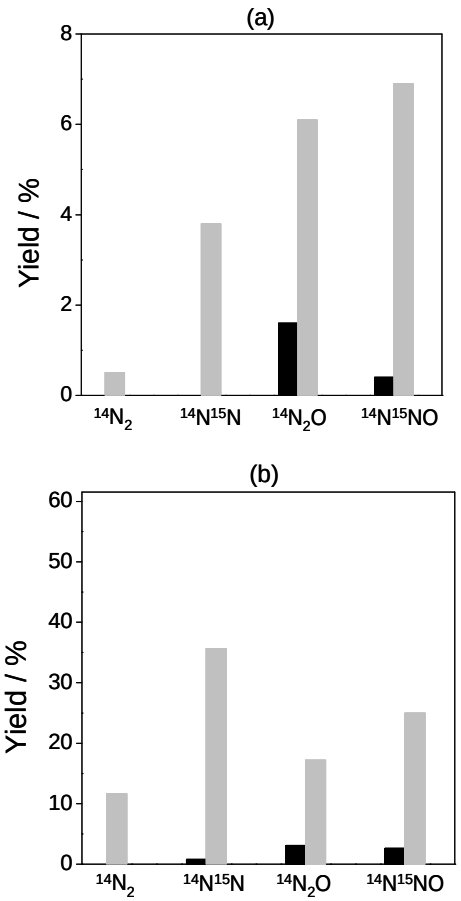

Fig.3: Yields of reaction products upon simultaneous pulsing of O_2/Xe = 1/1 and $^{15}NH_3/^{14}NO$/Ne = 1/1/1 mixtures at 423 (a) and 623 (b) K over oxidized (black bars) and reduced (grey bars) catalyst.

respectively. Fig. 2 (a) clearly shows an increase in the Kubelka-Munk function characterized by a broad absorption at ca. 420 nm. This increase becomes more pronounced with an increase in temperature. The absorption in this region reflects the existence of nano-sized Ag clusters [5, 15]. Absorption within the region of 210-240 nm can be attributed to Ag^+ isolated ions on γ-Al_2O_3 whereas a shift to higher wavelength (260-370 nm) indicates clustering [5, 15]. According to this assignment, UV/vis spectra presented in Fig. 2 confirm (i) the existence of Ag^+ after preparation (absorption at about 240 nm) and (ii) reduction of nano-sized AgO_x species to metallic Ag ones (poorly resolved absorption between 300 and 370 nm). The reduced silver species are easily reoxidized in an O_2-containing flow even at 433 K (Fig. 2 (b)). Thus it can be stated that silver species on alumina are characterized by a high degree of heterogeneity, depending on the preparation conditions, but nevertheless, two main classes are clearly distinguishable: clusters in the size range of 3 to 5 nm (resolved by HRTEM and UV/vis) and $Ag^+/Ag_n^{\delta+}$ species (resolved by UV/vis). Not depending on the nature of species, oxidized ones are easily reduced by H_2, while reduced ones are reoxidized by O_2.

3.2. Transient experiments over Ag/Al_2O_3

The influence of the state (oxidized and reduced) of silver particles on product formation in the ^{14}NO-$^{15}NH_3$-O_2 interactions over pre-oxidized and pre-reduced $2Ag/Al_2O_3$ is shown in Fig. 3.. Both, for oxidized and reduced catalyst, $^{14}N_2$, $^{14}N^{15}N$, $^{14}N_2O$, and $^{14}N^{15}NO$ were identified as main nitrogen-containing reaction products. The presence of nitrogen atoms originating from ammonia ($^{15}NH_3$) and from nitric oxide (^{14}NO) in nitrogen ($^{14}N^{15}N$, $^{14}N_2$) and nitrous oxide ($^{14}N^{15}NO$, $^{14}N_2O$) indicates that these products formally originate from only one type of N-containing feed molecules as well as from both types. Possible reaction pathways leading to differently labeled nitrogen and nitrous oxide are discussed in section 3.4 taking into account the results of our in situ IR analysis (section 3.3).

It is important to highlight that the amount of $^{14}N_2$, $^{14}N^{15}N$, $^{14}N_2O$, and $^{14}N^{15}NO$ over reduced silver particles is considerably higher than over oxidized ones. This means that the reduced silver particles are very active in the NH_3-SCR reaction. These results agree well with earlier mentioned steady-state catalytic performance of variously loaded Ag/Al_2O_3 catalysts [9], when the NH_3-SCR reaction was performed in the presence of H_2. A detailed analysis of the role of reduced and oxidized silver species in NH_3-NO, NH_3-NO-O_2 and NH_3-NO-O_2-H_2 interactions has been previously reported by us [10]. In the present study we particularly analyzed the role of hydrogen in N_2O and N_2 formation.

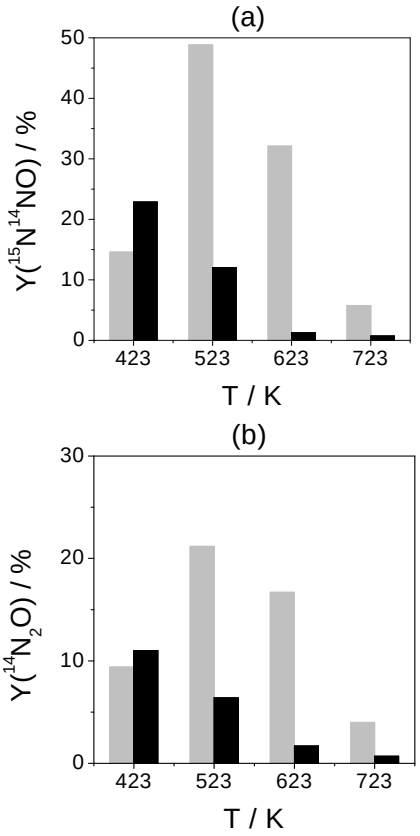

Fig. 4: Yields of $^{15}N^{14}NO$ (a) and $^{14}N_2O$ (b) upon pulsing $^{15}NH_3$-^{14}NO-O_2 (grey bars) and $^{15}NH_3$-^{14}NO-O_2-H_2 (black bars) over $2Ag/Al_2O_3$ at different temperatures.

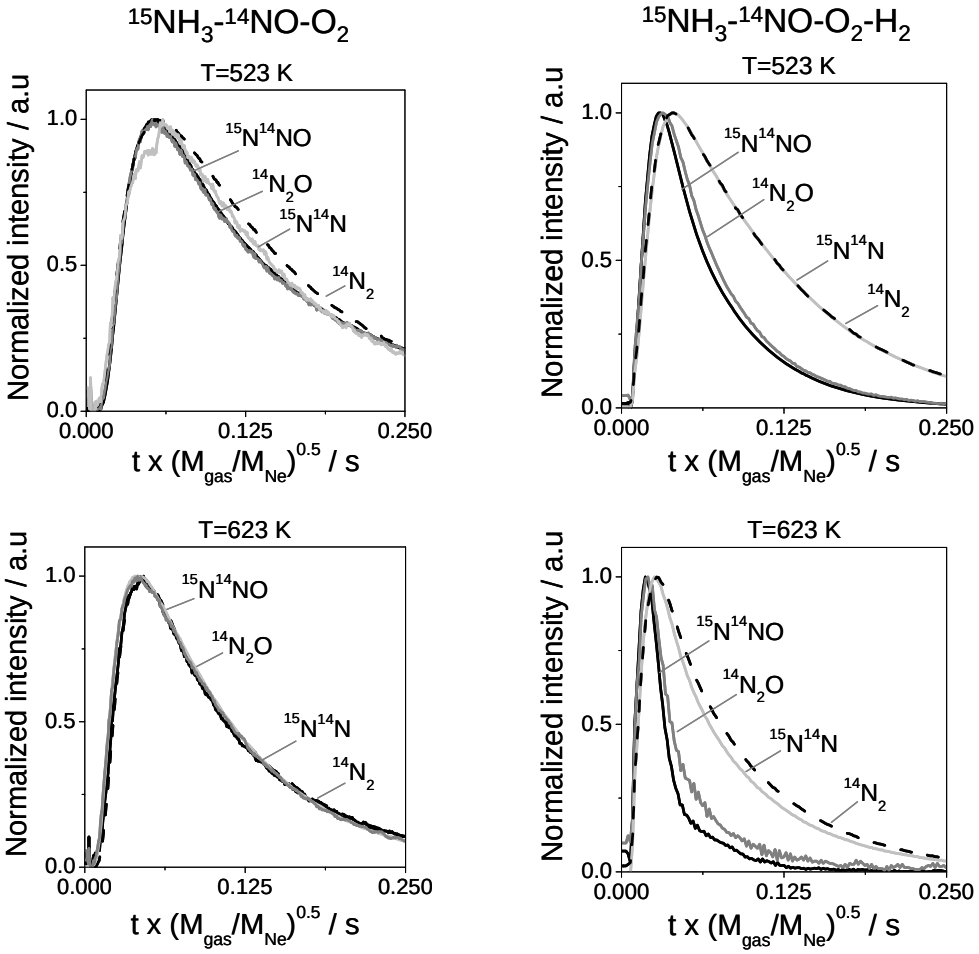

Fig. 5: Normalized transient responses of $^{14}N^{15}NO$, $^{14}N_2O$, $^{14}N^{15}N$ and $^{14}N_2$ after simultaneous pulsing of O_2/Xe = 1/1 and $^{15}NH_3/^{14}NO/H_2$/Ne = 1/1/10/1 mixtures over $2Ag/Al_2O_3$ at 523 (a) and 623 (b) K.

In agreement with steady-state catalytic tests [13], N_2O formation significantly decreases, when H_2 is added to an NH_3-NO-O_2 reaction mixture (Fig. 4). In order to elucidate possible mechanistic origins of this hydrogen effect onN_2O production we analyzed the shapes of transient responses of N_2O and N_2 recorded during experiments with two mixtures: i) NH_3-NO-O_2 and ii) NH_3-NO-O_2-H_2. According to the theory of the TAP [14], the shape of transient responses contains mechanistic information on chemical processes occurring on the catalyst, like sequence of product formation. For easier comparison of the shapes of transient responses of N_2O and N_2, they were normalized according to [14]. This procedure enables to compare the order of the appearance of gas-phase components, which differ significantly in their molecular weights.

The normalized transient responses of $^{14}N^{15}NO$, $^{14}N_2O$, $^{14}N^{15}N$ and $^{14}N_2$ recorded after simultaneous pulsing of $^{15}NH_3/^{14}NO$/Ne = 1/1/1 and O_2/Xe = 1/1 mixtures at 523 and 623 K are shown in Fig. 5. This figure illustrates that there are no significant differences in the shapes of N_2 ($^{14}N^{15}N$ and $^{14}N_2$) and N_2O ($^{14}N^{15}NO$, $^{14}N_2O$) transient responses in absence of H_2. The similar shapes of these normalized transient responses indicate that differently labeled nitrous oxide and nitrogen molecules are formed via parallel reaction pathways. This conclusion is not valid, when $^{15}NH_3$-^{14}NO-O_2 transient experiments are performed in the presence of hydrogen. Fig. 5 nicely shows a significant sharpening of the transient responses of $^{14}N^{15}NO$ and $^{14}N_2O$, when H_2 was pulsed together with ^{14}NO, $^{15}NH_3$ and O_2. For example at 623 K, the widths of normalized transient responses of nitrous oxide at their half height are 0.081 s and 0.023 s without and with H_2, respectively. Moreover, the maxima (t_{max}) of normalized transient responses of nitrous oxide are shifted to shorter times as compared to those of nitrogen: t_{max} of nitrous oxide is ca. 0.018 s, while t_{max} of nitrogen is ca. 0.043 s. Such a decrease in the t_{max} of nitrous oxide but an increase in the t_{max} of nitrogen, is due to the decomposition of primarily formed nitrous oxide to nitrogen. In principle, this conclusion is valid for $^{14}N^{15}NO$, $^{14}N_2O$, $^{14}N^{15}N$ and $^{14}N_2$. However, the transient responses of nitrogen and nitrous oxide containing two types of N-atoms ($^{14}N^{15}N$ and $^{14}N^{15}NO$) are slightly stronger influenced by the presence of H_2 as compared to those containing only ^{14}N-atoms (Fig. 5). This result indirectly supports our assumption that there are two different pathways leading to product molecules with and without labeled (^{15}N) nitrogen atoms.

In order to elucidate the possible role of surface intermediates in the formation of differently labeled nitrogen

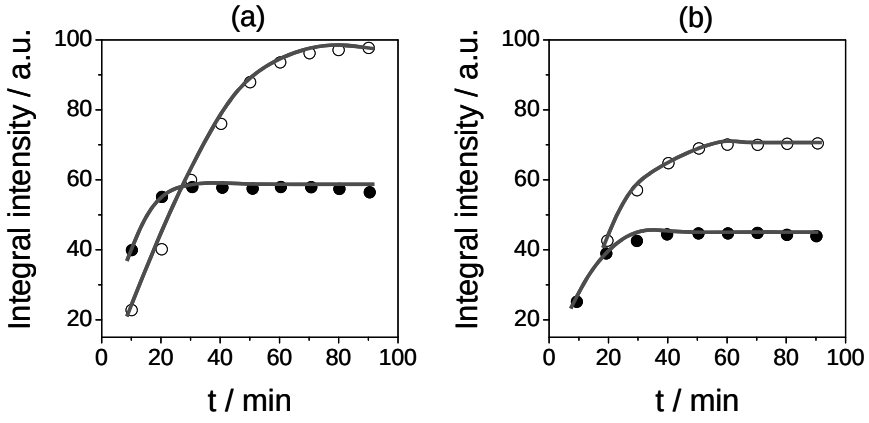

Fig. 6: Integral band intensities (1563 cm^{-1}) of nitrato species formed during interaction with 0.04 vol.% NO / 0.04 vol.% NH_3 / 4 vol.% O_2 (open circles) and 0.04 vol.% NO / 0.04 vol.% NH_3 / 4 vol.% O_2 / 1vol.% H_2 (full circles) on pre-oxidized (a) and pre-reduced (b) $2Ag/Al_2O_3$ catalyst at 423 K in dependence on time.

and nitrous oxide, we performed FTIR analysis. The results are presented and discussed below.

3.3. Surface intermediates

As shown in our previous study [18], nitrato species were formed upon NO/O_2 adsorption over variously loaded Ag/Al_2O_3 catalysts. The concentration of these adsorbed species increased in the presence of H_2. However, these nitrato species are only characteristic for the pre-oxidized sample, whereas unstable but reactive nitrite and nitro species were formed on the pre-reduced catalyst.

The exposure of the pre-oxidized catalyst to a gas mixture of 0.04 vol.% NO/0.04 vol.% NH_3/4 vol.% O_2 led to the formation of chelating bidentate nitrato species. Fig. 6(a) illustrates time-on-stream dependence of the concentration of these species over oxidized $2Ag/Al_2O_3$ in the absence and presence of H_2. One can see that this concentration increases with time in the absence of H_2. When H_2 is added to an $NO\text{-}NH_3\text{-}O_2$ feed the overall concentration of chelating bidentate nitrato species is significantly lower and reaches a constant value after 20 min on stream. The same effect was also found for the pre-reduced catalyst, however, the amount of nitrato species was essentially lower both during reaction with the H_2-free and the H_2-containing gas mixture (Fig. 6 (b)). In order to investigate whether these species react with ammonia, the pre-oxidized $2Ag/Al_2O_3$ catalyst was exposed to an NO/O_2 atmosphere followed by replacing of the oxidizing atmosphere with a reducing one. For comparison, besides 0.4 vol.% NH_3/Ar also 1 vol.% H_2/Ar was employed as reducing gas mixture. FTIR spectra recorded after different treatments are shown in Fig. 7. The broad bands around 1290 cm^{-1} and 1560 cm^{-1} in the spectra obtained after NO/O_2 adsorption are typical for chelating bidentate nitrato species. The intensity of these bands decreases after the exposure of the catalyst to H_2 and NH_3 indicating that these nitrato species react with both, hydrogen and ammonia. The interaction with H_2 does not lead to the formation of new ad-species. However, during exposure to ammonia the formation of new type of adsorbed species is reflected by the appearance of a new band at 1394 cm^{-1} and broadened bands at 1558 and 1303 cm^{-1}, which can be attributed to adsorbed NH_2NO or HNO [19]. These adsorbed species are stable only in the presence of gas phase. Their concentration strongly decreases upon evacuation at 796 K. After evacuation, bands at 1558, 1453, 1406 and 1303 cm^{-1} remain. The intensive bands at 1558/1303 indicate the presence of nitrato species. The low-intensity band at 1453 cm^{-1} results from nitrite species. The band at 1406 can be assigned to NH_4^+ (additional bands in the 3300-3200 cm^{-1} region), resulting from the reaction of NH_3 with formed water. In summary, the FTIR analysis has shown that ammonia reacts in a specific way with chelating bidentate nitrato species yielding NH_2NO or HNO species.

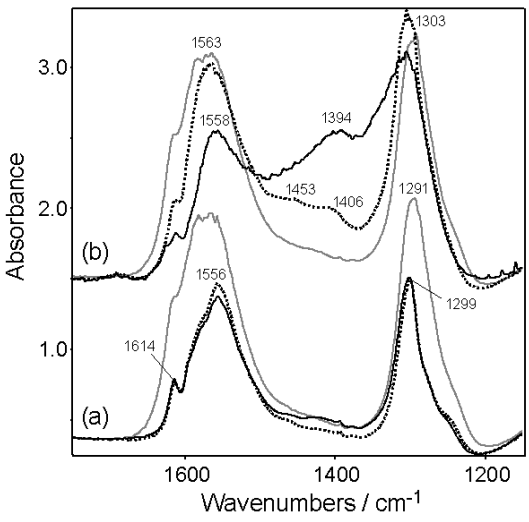

Fig. 7: FTIR spectra obtained after 30 min pre-adsorption of 0.09 vol.% NO/2 vol.% O_2 (grey lines), followed by exposure to 1 vol.% H_2/Ar (a) or 0.4 vol.% NH_3/Ar (b) for 60 min (black solid lines) and evacuation (dotted lines) at 423K, respectively.

3.4. Mechanistic aspects of the NH_3-SCR reaction in the absence and presence of O_2

Based on the results reported here and in our previous papers [10, 13], an improved mechanistic concept of the effect of oxygen and hydrogen on nitrogen and nitrous oxide formation in the NH_3-SCR over Ag/Al_2O_3 catalysts has been developed. A simplified scheme with the reaction network and product formation is illustrated in Fig.8. The scheme considers reaction pathways of N_2 and N_2O formation as well as factors governing activity and selectivity of the catalyst. Black arrows represent major reaction pathways, while the grey ones are for minor reactions. Reduced (Ag) and oxidized (AgO_x) silver species are supposed to be potential active sites in the NH_3-SCR reaction. In agreement with previous studies [9, 10, 13], the present results proved the low activity of oxidized AgO_x species for the reaction below 723 K. The reason for the lack of activity is the inability of lattice oxygen species of AgO_x aggregates to remove hydrogen atoms from NH_3 molecules yielding highly reactive surface NH_x fragments essential for further NO conversion. Reduced silver species formed upon reduction of oxidized AgO_x species with H_2 at temperatures above 373 K reveal, however, moderate activity towards NO reduction by NH_3 in the absence of gas-phase O_2 as it was observed during pulse experiments with $^{15}NH_3$-^{14}NO mixture [10]. This is due to the inertness of silver in ammonia activation, i.e. in breaking N-H bonds in the ammonia molecule [20]. Stripping of hydrogen atoms from NH_3 molecules requires, therefore, participation of oxygen species. The oxygen species active in the formation of NH_x from NH_3 are denoted in the scheme as Ag-O_{ads} (Fig. 8). Concerning the nature of active oxygen species, it is well established that, depending on reaction conditions, interaction of oxygen with silver catalysts results in stabilization of various adsorbed molecular and atomic oxygen species [21-25]. Molecularly adsorbed oxygen species exist on the surface between 25 and 170 K. At higher temperatures oxygen molecules dissociate to atomically adsorbed species, which recombine and desorb above ca. 500 K. Penetration of oxygen atoms into bulk of metallic silver or formation of oxide layers are accelerated upon increasing reaction temperature and oxygen partial pressure [23, 25]. Due to the variety of oxygen species on silver, which can exist on the catalyst surface in the studied temperature range, it is not possible at this stage to precisely identify the nature of oxygen species responsible for the dehydrogenation of ammonia.

Since the amount of reaction products in the NH_3-NO interactions over reduced Ag species is considerably enhanced in the presence of gas-phase O_2 [10], it is concluded that molecular oxygen generates either more reactive surface oxygen species than NO does, and/or the concentration of oxygen species is considerably higher. Based on the experimental results on distribution of ^{14}N and ^{15}N in nitrogen and nitrous oxide [10], it is concluded that NO cannot be effectively decomposed over reduced Ag species with formation of N_2, N_2O and active oxygen species. This statement is supported by previous surface science studies [26, 27], which reported low activity of metallic silver for NO dissociation. More typical for this metal, especially in the presence of oxygen, is the formation of NO_2 and NO_3 surface species. Depending on the reaction conditions the latter can form layers of surface nitrate [26].

Ammonia fragments (Ag-NH_x,Fig. 8) resulting from the interaction of active adsorbed oxygen species with NH_3 are essential for the formation of surface NH_2NO species identified by FTIR (Fig. 7). This surface species is a possible intermediate of gas-phase nitrogen and nitrous oxide formation. The isotopic distribution of nitrogen atoms in these products in $^{15}NH_3$-^{14}NO-H_2-O_2 interactions indirectly supports the participation of surface NH_2NO species in the formation of gas-phase products. As shown in our previous paper [10] and in Fig. 3 $^{15}N^{14}N$ and $^{15}N^{14}NO$ are the main nitrogen-containing products of ^{14}NO reduction by $^{15}NH_3$, i.e. these products are formed via a coupling reaction of $^{15}NH_3$ and ^{14}NO. Moreover, $^{15}N^{14}N$ is the main nitrogen-containing product formed upon O_2 pulsing over the catalyst having been treated by $^{15}NH_3$-^{14}NO-O_2 mixture at 723 K. The latter result strongly supports the conclusion that adsorbed $^{15}NH_3$- and ^{14}NO- containing species are decomposed by O_2 yielding gas-phase nitrogen. Since there is a correlation between the composition of gas-phase products and the presence of adsorbed NH_2NO species we suggest that these species are intermediates in the NO reduction by NH_3. Participation of adsorbed HNO, as alternative intermediate, in the formation of N_2O and N_2 seems to be doubtful, since no indication of such adsorbates was observed in FTIR spectra during switch from NO/O_2 to H_2/Ar mixture, although direct formation of these species could be expected. Moreover, recombination of two HNO species predicts dominant formation of nitrogen and nitrous oxide molecules containing only one type of nitrogen atoms. However, $^{14}N^{15}N$ and $^{14}N^{15}NO$ were mainly formed during experiments with $^{15}NH_3$-^{14}NO-O_2 and $^{15}NH_3$-^{14}NO-O_2-H_2 mixtures over reduced catalyst [10]. Therefore, it was assumed that surface NH_2NO species are the major intermediates participating in the formation of N_2 and N_2O over the catalyst studied. The importance of NH_x-NO surface complexes in N_2 and N_2O formation have tentatively mentioned for low-temperature [28] and high-temperature NH_3-NO-O_2 interactions [29] over Pt-based catalysts.

Based on the isotopic distribution of reaction products shown in Fig. 3, it can be concluded that the decomposition of NH_2NO species is not the only reaction pathway leading to nitrogen and nitrous oxide. The formation of $^{14}N_2O$, formally originated from two ^{14}NO feed molecules can be attributed to the recombination of two adsorbed NO species as reported for silver catalysts supported on Al_2O_3 [30]. However, this reaction pathway is less important in comparison to the decomposition of NH_2NO species.

Similarly it can be expected that recombination of nitrogen atoms originating from dissociated NO species and NH_3 molecules, which passed through the whole stripping sequence (NH_2 – NH – N), also contribute to the total ni

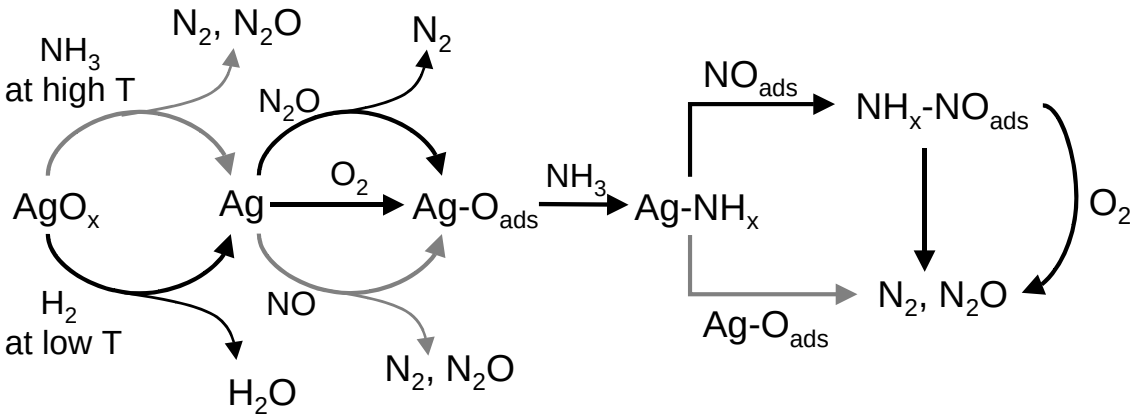

Fig. 8: Reaction network of the NH_3-SCR reaction over $2Ag/Al_2O_3$.

trogen formation. However, the present study evidenced that in the presence of hydrogen other reaction pathways play a significant role. As it was concluded from the analysis of the shapes of the transient responses of N_2O and N_2 obtained during studies of $^{15}NH_3$-^{14}NO-O_2-H_2 interactions (Fig. 5), in addition to the transformation of surface NH_2NO species to N_2, N_2 originates via N_2O decomposition over reduced Ag particles. This experimental observation agrees well with previous suggestions of Burch et al. [31]. These authors studied the influence of H_2 on N_2O decomposition over a Pt/SiO_2 catalyst in the temperature range from 473 to 773 K. They explained the boosting effect of H_2 on N_2O decomposition by i) an H-assisted N_2O dissociation mechanism and ii) by the removal of "hot" oxygen species formed from N_2O through adsorbed hydrogen species. The latter process leads to the regeneration of reduced metallic sites active for N_2O decomposition. However, it should be noted that in NO reduction by ammonia, oxygen species originating from N_2O decomposition could participate in ammonia activation. Probably, hydrogen interacts with oxygen species yielding OH groups, which are more effective for NH_3 activation as adsorbed oxygen atoms at least on Pt and Rh catalysts [32, 33].

Thus, the mechanistic effects of H_2 and O_2 on product formation in NH_3-SCR over $2Ag/Al_2O_3$ can be summarized as follows. H_2 is required for the reduction of AgO_x at low temperatures (above 373 K) yielding reduced Ag species. The reduced Ag species catalyze generation of active oxygen species from O_2 and decomposition of primarily formed N_2O yielding gas-phase N_2 and surface oxygen species. The formed oxygen species participate in ammonia dehydrogenation yielding reactive NH_x fragments. The latter accelerate NO conversion to N_2 and N_2O via thermal or O_2-assisted decomposition of surface NH_2NO species.

4. Conclusions

The mechanistic information obtained in the present study together with previously published results allowed to develop an improved mechanistic scheme of NO reduction with NH_3 to N_2 and N_2O in the presence of O_2 and H_2. The results presented in this paper highlight the importance of reduced Ag species for performance of $2Ag/Al_2O_3$ in NH_3-NO interactions. In situ UV/vis spectroscopy and HRTEM enabled to detect the reduction of AgO_x to metallic Ag starting at 373 K in a hydrogen-containing flow. The reduced Ag species decompose NO to N_2 and N_2O as well as N_2O to N_2. However, the main reaction pathway leading to N_2 and N_2O is direct or oxygen-induced decomposition of surface NH_2NO species. These surface species are formed from NO and adsorbed NH_2 fragments, which originate from ammonia activation by adsorbed oxygen species resulting mainly from O_2 dissociation over reduced Ag species.

References

1. S. Satokawa, Chem. Lett., 29 (2000) 294.
2. S. Satokawa, J. Shibata, K.-i. Shimizu, A. Satsuma, T. Hattori, Appl. Catal. B, 42 (2003) 179.
3. J. Shibata, K.-i. Shimizu, Y. Takada, A. Shichi, H. Yoshida, S. Satokawa, A. Satsuma, T. Hattori, J. Catal., 227 (2004) 367.
4. S. Satokawa, J. Shibata, K.-i. Shimizu, A. Satsuma, T. Hattori, T. Kojima, Chem. Eng. Sci., 62 (2007) 5335.
5. P. Sazama, L. Capek, H. Drobna, Z. Sobalik, J. Dedecek, K. Arve, B. Wichterlova, J. Catal., 232 (2005) 302.
6. K.-I. Shimizu, A. Satsuma, J. Phys. Chem., 111 (2007) 2259.
7. R. Brosius, K. Arve, M.H. Groothaert, J.A. Martens, J. Catal., 231 (2005) 344.
8. J. Shibata, Y. Takada, A. Shichi, S. Satokawa, A. Satsuma, T. Hattori, J. Catal., 222 (2004) 368.
9. M. Richter, U. Bentrup, R. Eckelt, M. Schneider, M.-M. Pohl, R. Fricke, Appl. Catal. B, 51 (2004) 261.

10. E.V. Kondratenko, V.A. Kondratenko, M. Richter, R. Fricke, J. Catal., 239 (2006) 23.
11. B. Wichterlova, P. Sazama, J.P. Breen, R. Burch, C.J. Hill, L. Capek, Z. Sobalik, J. Catal., 235 (2005) 195.
12. N. Bion, J. Saussey, M. Haneda, M. Daturi, J. Catal., 217 (2003) 47.
13. M. Richter, R. Fricke, R. Eckelt, Catal. Lett., 94 (2004) 115.
14. J.T. Gleaves, G.S. Yablonsky, P. Phanawadee, Y. Schuurman, Appl. Catal. A, 160 (1997) 55.
15. M. Richter, A. Abramova, U. Bentrup, R. Fricke, J. Appl. Spectrosc., 71 (2004) 368.
16. K.-I. Shimizu, M. Tsuzuki, K. Kato, S. Yokota, K. Okumura, A. Satsuma, J. Phys. Chem. C, 111 (2007) 950.
17. J.P. Breen, R. Burch, C. Hardacre, C.J. Hill, J. Phys. Chem. B, 109 (2005) 4805.
18. U. Bentrup, M. Richter, R. Fricke, Appl. Catal. B, 55 (2005) 213.
19. G. Ramis, L. Yi, G. Busca, M. Turco, E. Kotur, R.J. Willey, J. Catal., 157 (1995) 523.
20. D.M. Thornburg, R.J. Madix, Surf. Sci., 220 (1989) 268.
21. C.T. Campbell, Surf. Sci., 157 (1985) 43.
22. M. Dean, A. McKee, M. Bowker, Surf. Sci., 211/212 (1989) 1061.
23. X. Bao, M. Muhler, T. Schedel-Niedrig, R. Schlögl, Phys. Rev. B, 54 (1996) 2249.
24. A. Nagy, G. Mestl, T. Rühle, G. Weinberg, R. Schlögl, J. Catal., 179 (1998) 548.
25. D.Y. Zemlyanov, A. Nagy, R. Schlögl, Appl. Surf. Sci., 133 (1998) 171.
26. D. Zemlyanov, R. Schlögl, Surf. Sci., 470 (2000) L20.
27. X. Bao, U. Wild, M. Muhler, B. Pettinger, R. Schlögl, G. Ertl, Surf. Sci., 425 (1999) 224.
28. K. Otto, M. Shelef, J.T. Kummer, J. Phys. Chem., 74 (1970) 2690.
29. J. Pérez-Ramírez, E.V. Kondratenko, V.A. Kondratenko, M. Baerns, J. Catal., 229 (2005) 303.
30. J. Muslehiddinoglu, M.A. Vannice, J. Catal., 217 (2003) 442.
31. R. Burch, S.T. Daniells, J.P. Breen, P. Hu, Catal. Lett., 94 (2004) 103.
32. M. Baerns, R. Imbihl, V.A. Kondratenko, R. Kraehnert, W.K. Offermans, R.A. van Santen, A. Scheibe, J. Catal., 232 (2005) 226.
33. C. Popa, R.A. van Santen, A.P.J. Jansen, J. Phys. Chem., 111 (2007) 9839.